Heliyon 10 (2024) e26739

Contents lists available at ScienceDirect

Heliyon

journal homepage: www.cell.com/heliyon

Research article

Transcriptomics analyses of IL-1β-stimulated rat chondrocytes in temporomandibular joint condyles and effect of platelet-rich plasma

Shasha Liu [a,b,*], Chaolun Wu [a], Yuxin Zhang [a]

[a] Department of Rehabilitation Medicine, The Ninth People's Hospital, Shanghai Jiao Tong University School of Medicine, Shanghai, 200011, China
[b] Department of Rehabilitation Medicine, Sijing Hospital of the Songjiang District of Shanghai, Shanghai, 201600 China

ARTICLE INFO

Keywords:
Chondrocytes
Interleukin-1 beta
Platelet-rich plasma
Temporomandibular joint

ABSTRACT

The biological mechanism of action of platelet-rich plasma (PRP) in the treatment of temporomandibular joint (TMJ) osteoarthritis remains unclear. This study explored the mechanisms underlying interleukin (IL)-1β-induced inflammation and investigated the effect of PRP on TMJ condylar chondrocytes. Primary chondrocytes were isolated from the TMJ condyle of 4-week-old rats, and differentially expressed genes among three treatment groups (phosphate-buffered saline [control], IL-1β, and IL-1β + PRP) were identified using RNA-seq and characterized using Gene Ontology and Kyoto Encyclopedia of Genes and Genomes path-enrichment analyses. IL-1β caused inflammatory injury to chondrocytes by upregulating the TNF, NF-κB, and IL-17 signaling pathways and downregulating the MAPK and PI3K/Akt signaling pathways. PRP activated the MAPK and PI3K/Akt signaling pathways, exerting a protective effect on IL-1β-induced chondrocytes. PRP also activated the TNF and IL-17 signaling pathways, producing an inflammatory effect. Additionally, PRP increased the mRNA expression of the matrix catabolism-related genes *Mmp3*, *Mmp9*, and *Mmp13*; the proliferative markers Mki67 and PCNA; and the anti-apoptotic genes of the Bcl-2 family (*Bcl2a1* and *Bok*), while reducing the expression of the pro-apoptotic genes *Casp4* and *Casp12*. The findings suggest that the protective effect of PRP on IL-1β-induced chondrocyte injury is mainly achieved via MAPK-PI3K/Akt signaling, increasing cell proliferation and inhibiting cell apoptosis.

1. Introduction

The temporomandibular joint (TMJ) is a bilateral synovial joint that orchestrates one of the most intricate and complex movements of all human joints [1] and is closely involved in various important functions such as chewing, swallowing, speech, and facial expression. TMJ osteoarthritis (TMJ-OA) is characterized by degenerative changes in the condylar bone such as cortical erosion, subcortical cystic changes, osteophyte formation, and sclerosis [2]. According to radiological assessments, the prevalence of TMJ-OA in the general population ranges from 8% to 30% [3]. The main clinical manifestations include orofacial pain, crepitus, and limited joint movement [4]. The most common risk factors for TMJ-OA include sex, mechanical stress (dental malocclusion, parafunction, and

* Corresponding author. Department of Rehabilitation Medicine, The Ninth People's Hospital, Shanghai Jiao Tong University School of Medicine, Shanghai, 200011, China.
E-mail address: shuiliushasha@foxmail.com (S. Liu).

https://doi.org/10.1016/j.heliyon.2024.e26739
Received 23 November 2023; Received in revised form 9 February 2024; Accepted 19 February 2024
Available online 20 February 2024

disc placement), and advanced age [5,6]. Multiple inflammatory cytokines may play important roles in the pathogenesis of TMJ-OA. The mRNA levels of interleukin (IL)-1β, IL-2, IL-12, IL-17, IL-18, TNF-α, TNF-β, and IFN-γ in the synovial fluid from the TMJ in patients with TMJ-OA were found to be significantly higher than those in healthy individuals [7]. The expression of IL-1β and TNF-α have been reported to be related to cartilage degradation and the inhibition of cartilage matrix synthesis in TMJ-OA [8]. The production and activation of matrix metalloproteinases (MMPs) by fibrochondrocytes have also been shown to be involved in inflammation-induced matrix degradation [9,10]. However, the pathogenesis of TMJ-OA remains unclear.

Although physical therapy and/or treatment with paracetamol and non-steroidal anti-inflammatory drugs can temporarily alleviate inflammatory symptoms [11], they fail to prevent or slow down disease progression. This highlights the urgent need to identify effective therapeutic targets and methods. The joint cartilage is mainly composed of chondrocytes and extracellular matrix (ECM), with chondrocytes regulating ECM formation or degradation via synthetic or catabolic factors [12]. Condylar chondrocytes are important for maintaining the stability of normal TMJ cartilage, and inflammation-induced death of condylar chondrocytes and degradation of articular cartilage are closely related to the occurrence and development of TMJ-OA [13,14]. Therefore, protecting chondrocytes to enhance proliferation and inhibition of apoptosis appears to be a highly promising strategy for effective TMJ-OA treatment.

Platelet-rich plasma (PRP) is an autologous blood product obtained through centrifugation. PRP, which is characterized by highly concentrated platelets, can exhibit platelet concentrations that are three to five times higher than those in human plasma [15,16]. As one of the current core technologies used in rehabilitation and regeneration therapy, the usefulness of PRP therapy has recently been confirmed through many laboratory and clinical studies that demonstrated its effectiveness in ameliorating the symptoms of OA and repairing cartilage defects [17,18]. Multiple clinical studies have found that the injection of PRP not only effectively alleviates pain and joint noise in patients with TMJ-OA, but also improves mandibular function and repairs the condylar bone, as verified by imaging [19–22]. A previous study reported that PRP affected cartilage thickness by inhibiting chondrocyte apoptosis in OA [23]. However, the biological mechanism of action of PRP in the treatment of TMJ-OA has not been clearly elucidated yet. Therefore, we conducted a transcriptome analysis to investigate the mechanism of chondrocyte inflammatory injury in TMJ-OA and characterize the mechanism

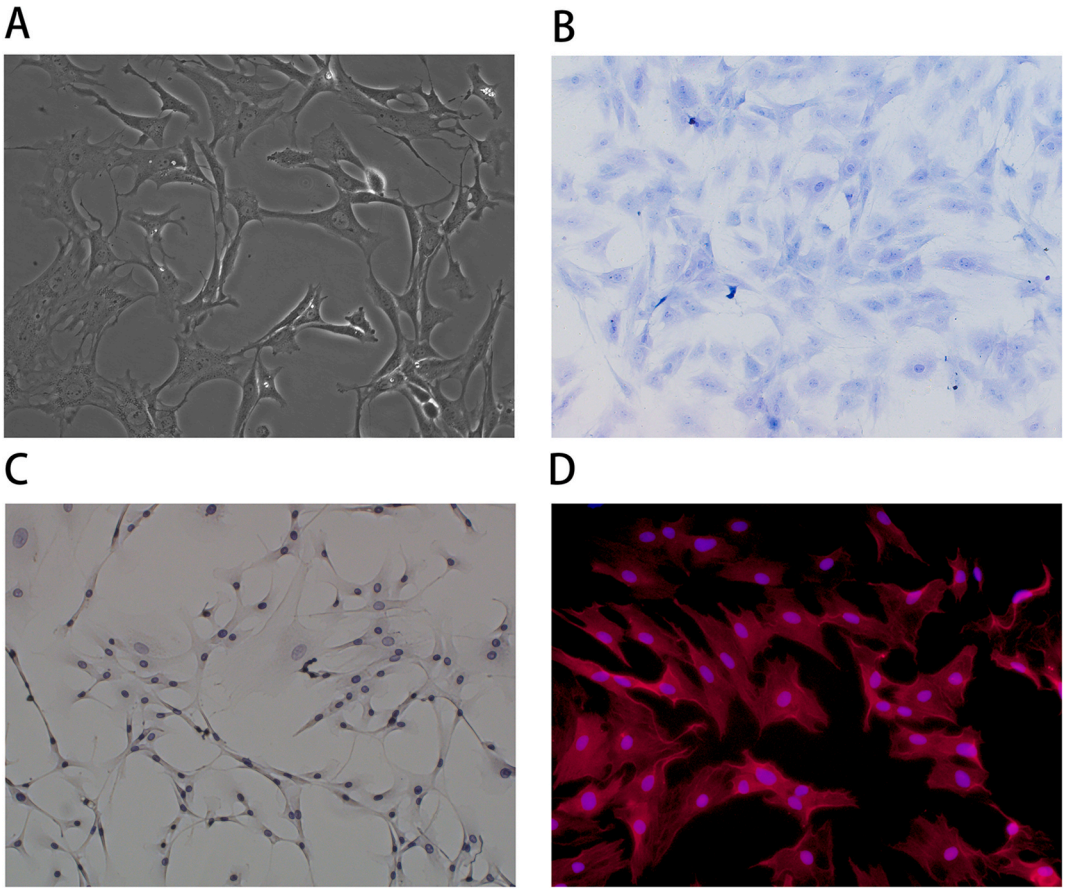

Fig. 1. Chondrocyte purity assessment. (A) Inverted phase contrast microscopy imaging of chondrocytes (magnification, × 200). (B) Chondrocytes identified using Alcian Blue staining (magnification, × 200). (C) Chondrocytes identified using immunocytochemistry staining of type II collagen (magnification, × 200). (D) Chondrocytes identified using the immunofluorescence staining of type II collagen (magnification, × 200). (For interpretation of the references to colour in this figure legend, the reader is referred to the Web version of this article.)

by which PRP protects against inflammation-induced condylar chondrocyte injury.

2. Results

2.1. Identification of TMJ condylar chondrocytes

Primary condylar chondrocytes were extracted and seeded in a culture flask. The cells began to adhere to the wall after 4 h and entered a rapid proliferation phase after 3–5 days. Subsequently, P2 cells were identified as chondrocytes using toluidine blue (TB) staining, collagen II immunohistochemistry, and immunofluorescence staining (Fig. 1).

2.1.1. Effect of IL-1β on chondrocyte cell viability and of PRP on the viability of IL-1β-induced chondrocytes

Elevated expression of IL-1β was found in the TMJ of patients with TMJ-OA [7]. IL-1 can induce inflammation by activating the NF-κB signaling pathway and the Wnt signaling pathway mediating chondrocyte apoptosis, and by upregulating MMP-mediated ECM degradation [24,25]. In previous studies, IL-1β has been shown to induce injury to condylar chondrocytes [26]; therefore, this study used IL-1β to induce inflammatory chondrocytes.

Chondrocytes with an appropriate growth status were seeded into a 96-well plate at a density of 5×10^3 cells/well. After standard culture for 24 h, the cells were treated with IL-1β at different concentrations (0, 5, 10, and 20 ng/mL) for 6, 12, 24, 48, and 72 h. For each well, 10 μL of the Cell Counting Kit-8 (CCK-8, Beyotime, Shanghai, China) solution was added, and the sample was incubated at 37 °C for 1 h. Absorbance was measured at 450 nm using a spectrophotometer. The cell survival rates of the treated groups were then calculated.

Next, chondrocytes with an appropriate growth status were seeded into a 96-well plate at a density of 5×10^3 cells/well. After normal cultivation for 24 h, the cultured cells were treated with phosphate-buffered saline (PBS), 10 ng/mL of IL-1β, 10 ng/mL of IL-1β + 50 μg/mL PRP, or 10 ng/mL of IL-1β + 500 μg/mL PRP. Cell viability was measured using the CCK-8 method at 6, 12, 24, 48, and 72 h. The group treated with PBS was used as control, and the cell survival rates of each group were determined.

2.1.2. IL-1β-induced inflammatory state of condylar chondrocytes and signaling pathway prediction

As shown in Figs. 2 and 10 ng/mL IL-1β caused a stable decrease in cell survival rate within 24 h. Three groups of chondrocytes treated with PBS, 10 ng/mL IL-1β, or 10 ng/mL IL-1β + 500 μg/mL for 24 h were used for subsequent RNA extraction and transcriptome sequencing.

Transcriptome sequencing and functional annotation analysis, total RNA extraction, RNA library construction, and transcriptome

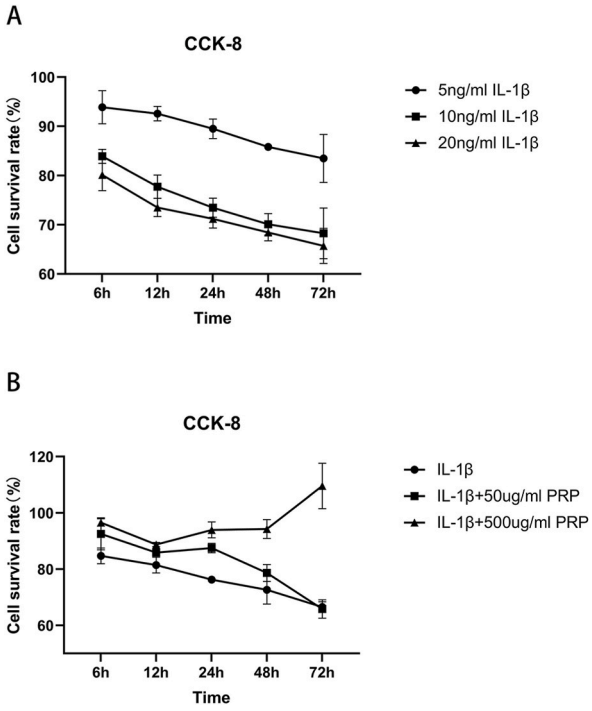

Fig. 2. Survival rate of chondrocytes treated with IL-1β and PRP determined using the Cell Counting Kit-8 method. (A) The survival rate of chondrocytes observed at 6, 12, 24, 48, and 72 h after treatment with IL-1β at concentrations of 5, 10, and 20 ng/mL. (B) The survival rates of chondrocytes observed at 6, 12, 24, 48, and 72 h after treatment with 10 ng/mL IL-1β, 10 ng/mL of IL-1β + 50 μg/mL PRP, and 10 ng/mL IL-1β + 500 μg/mL PRP.

sequencing were performed at Oebiotech (Shanghai, China). Gene Ontology (GO) and Kyoto Encyclopedia of Genes and Genomes (KEGG) analyses were performed to further understand the molecular basis of chondrocyte inflammation. The volcano plot on Fig. 3A shows differences in gene expression between inflammatory chondrocytes induced by IL-1β (n = 3) and normal chondrocytes, with log2 FoldChange and -log10q-value on the horizontal and vertical axes, respectively. A heat map was used for clustering, with red and blue indicating high- and low-expression genes, respectively (Fig. 3B). The radar map revealed 30 upregulated or downregulated genes

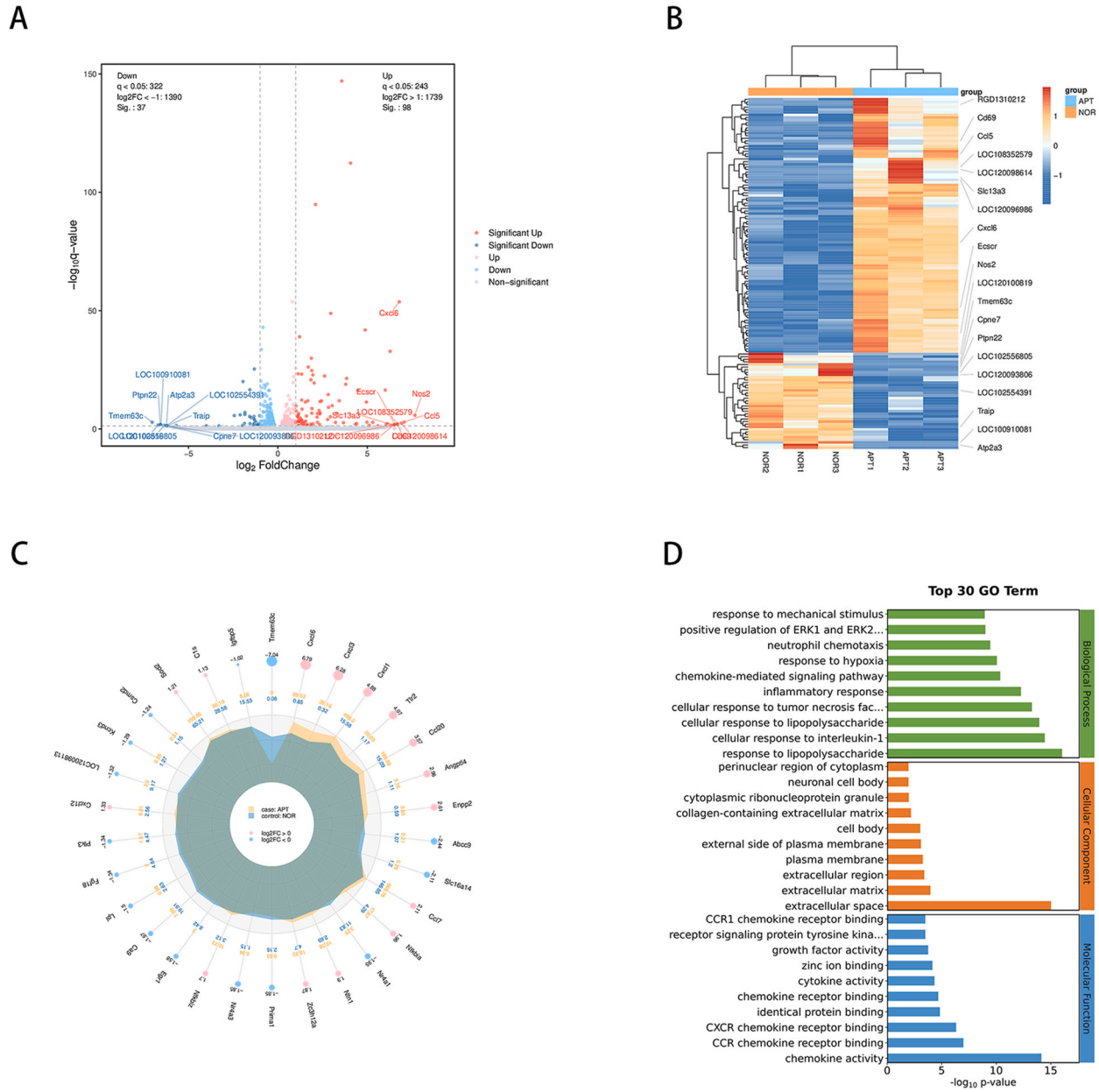

Fig. 3. Chondrocyte transcriptomic analysis of IL-1β-induced inflammation. (A) Volcano plot showing differential gene expression between control (n = 3) and IL-1β-induced chondrocytes (n = 3). Red indicates significantly upregulated genes (98), blue indicates significantly downregulated genes (37), and gray indicates no significant change (log2FoldChange [FC] > 1, padj <0.05). The horizontal and vertical axes are log2FC and - log10q-value, respectively. (B) Heat map showing the hierarchical clustering of differential gene expression in normal and inflammatory chondrocytes. (C) Radar map showing the 30 upregulated/downregulated genes with the lowest p-values. First circle: upregulated (red) and downregulated genes (blue). Circle size varies according to the size of log2 FC value. Second circle: the outer circle data represent the average expression level of the experimental group, and the inner circle data represent average expression level of the control group. Third circle: average expression level of each gene in the experimental and control groups. (D) Gene ontology (GO) enrichment analysis of differential gene expression between normal and inflammatory chondrocytes. GO enrichment analysis was performed on each of the three GO categories (BP, MF, and CC). (For interpretation of the references to colour in this figure legend, the reader is referred to the Web version of the article.)

with the lowest p-value (Fig. 3C).

After identifying the differentially expressed genes (DEGs), GO enrichment analysis was performed to determine their respective functions. The GO enrichment analysis for the top 30 entries (screened GO entries corresponding to PopHits ≥5 in the three classifications and ranked 10 entries in descending order according to the corresponding - log10p value of each entry) is shown in Fig. 3D. The KEGG database, which is the primary public pathway database [15], was used to conduct a pathway analysis of differentially-expressed protein-coding genes, and the hypergeometric distribution test method was used to calculate the significance of differential gene enrichment in each pathway entry. KEGG enrichment analysis was performed on the upregulated and downregulated genes, and the top 20 (selected pathway entries corresponding to PopHits ≥5, sorted based on the - log10p-value corresponding to each entry in descending order) bubble plots for each are shown in Fig. 4A and B, respectively.

2.1.3. PRP effects on IL-1β-induced inflammatory chondrocytes and signaling pathway prediction

Differential gene expression analysis was performed for two groups of chondrocytes treated with 10 ng/mL IL-1β or 10 ng/mL IL-1β + 500 μg/mL PRP. The volcano plot shows the differences in gene expression between IL-1β-induced inflammatory chondrocytes (n = 3) and IL-1β-induced inflammatory chondrocytes treated with PRP (n = 3) (Fig. 5A). Clustering analysis was performed using heat maps, with red and blue indicating high- and low-expressed genes, respectively (Fig. 5B). The radar map revealed 30 upregulated or downregulated genes with the lowest p-values (Fig. 5C).

After identifying the DEGs, GO enrichment analysis was performed to determine their respective functions. GO enrichment analysis of the top 30 entries was performed (the GO entries corresponding to PopHits ≥5 in the three classifications were screened, and 10 entries were ranked in descending order according to the corresponding log10p value of each entry); a bar chart is shown in Fig. 5D. KEGG enrichment analysis was performed on the upregulated and downregulated genes, and the top 20 (selected pathway entries corresponding to PopHits ≥5, sorted based on the - log10p value corresponding to each entry in descending order) bubble plots are shown in Fig. 6A and B.

Additionally, among the DEGs induced by PRP in inflammatory chondrocytes, 67 genes overlapped with the DEGs in chondrocytes induced by IL-1β during the inflammatory process (Fig. 7A and B). Among these, 33 genes were regulated in the opposite direction, whereas 34 genes were either upregulated or downregulated in both cases. The overlapping genes were mainly involved in interaction with cytokines (Fig. 7C).

2.1.4. Quantitative reverse transcription polymerase chain reaction (qRT-PCR) validation

The mRNA expression levels of the 10 TMJ-OA-related genes were verified using qRT-PCR (Table 1). Five of these genes were regulated in the opposite direction, whereas the regulation of the remaining five genes was in the same direction, as shown in Fig. 8. The qRT-PCR results were consistent with those of the transcriptomic sequencing. These 10 genes included those encoding nuclear receptor subfamily 4 group A member 1 (*Nr4a1*), polo-like kinase 3 (*Plk3*), ectonucleotide pyrophosphatase/phosphodiesterase 2 (*Enpp2*), interleukin 17B (*Il17b*), secreted frizzled related protein 1 (*Sfrp1*), interleukin 6 (*Il6*), TNF alpha induced protein 2 (*Tnfaip2*), TNF alpha induced protein 3 (*Tnfaip3*), matrix metallopeptidase 3 (*Mmp3*), and matrix metallopeptidase 3 (*Mmp9*).

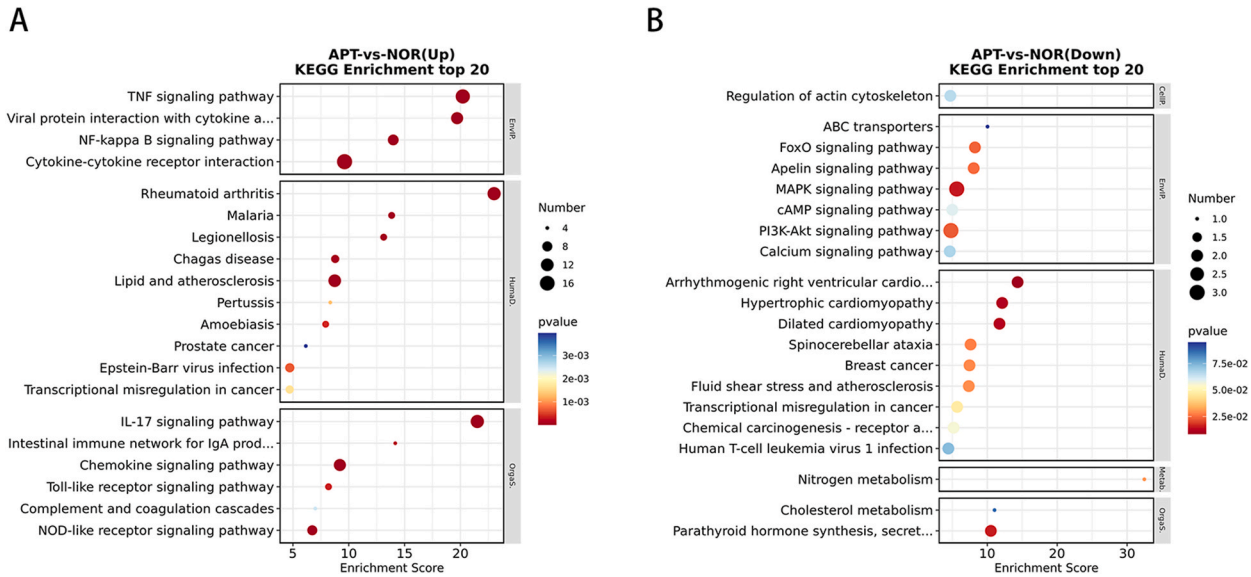

Fig. 4. Kyoto Encyclopedia of Genes and Genomes (KEGG) pathway analysis of interleukin (IL)-1β-induced inflammation. (A) KEGG pathway analysis of upregulated differentially expressed genes (DEGs) in control and inflammatory chondrocytes. (B) KEGG pathway analysis of downregulated DEGs in control and inflammatory chondrocytes.

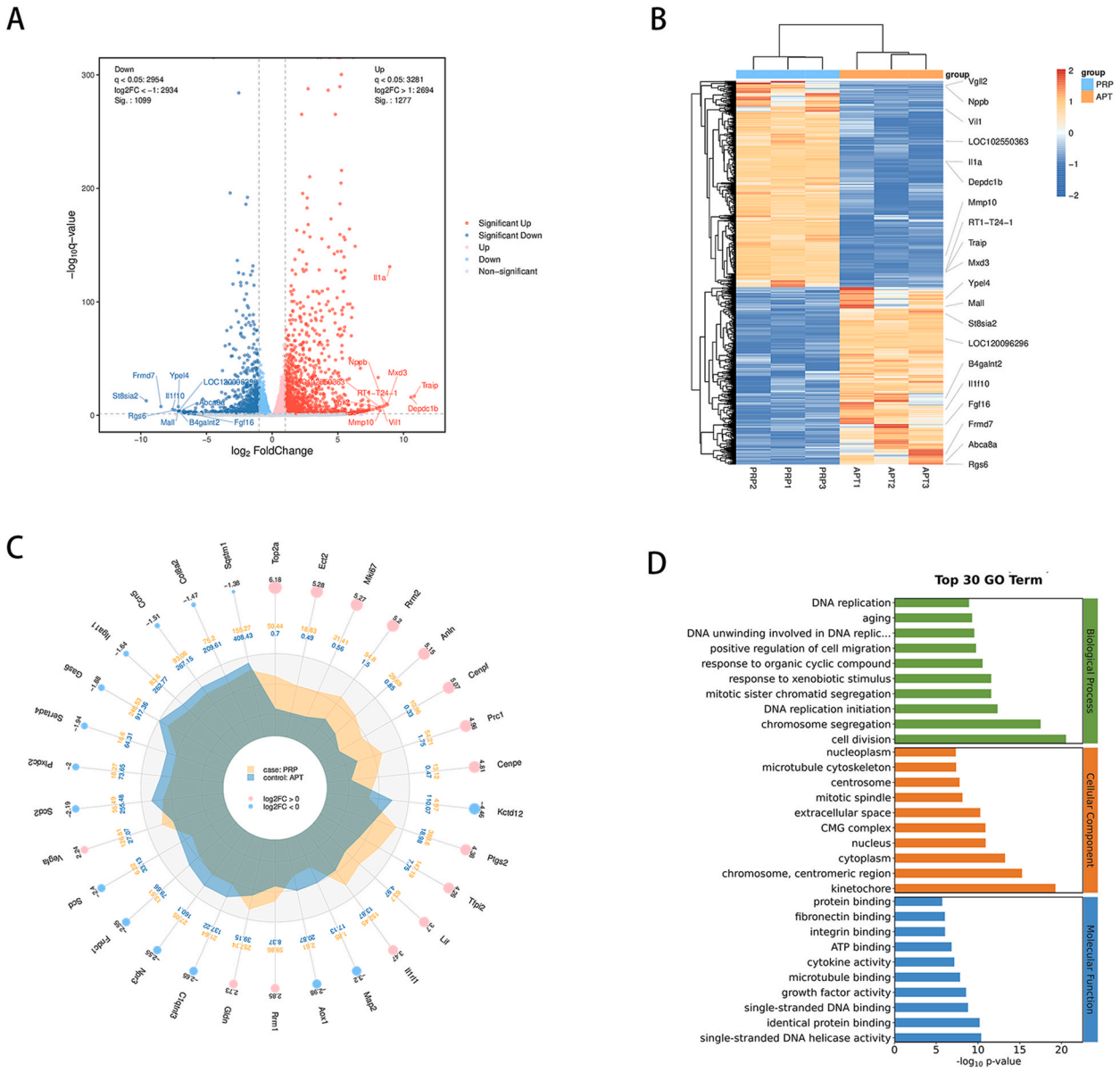

Fig. 5. Transcriptome analysis of the platelet-rich plasma (PRP) effect on interleukin (IL)-1β-induced inflammatory chondrocyte function. (A) Volcano plot showing differential gene expression between IL-1β-induced chondrocytes (n = 3) and IL-1β-induced chondrocytes treated with PRP (n = 3). Red indicates significantly upregulated genes (1,277), blue indicates significantly downregulated genes (1,099), and gray indicates no significant difference (log2 FoldChange [FC] > 1, padj <0.05). The horizontal and vertical axes correspond to the log2FC and - log10q-value, respectively. (B) Heat map showing the hierarchical clustering of differential gene expression in the two groups of chondrocytes. (C) Radar map showing the 30 upregulated and downregulated genes with the lowest p-value. First circle: upregulated genes (red) and downregulated genes (blue) Circle size varies according to the size of log2 FC value. Second circle: the outer circle data represent the average expression level of the experimental group and the average expression level of the control group, represented by the inner circle data. Third circle: the average expression level of each gene in the experimental and control groups. (D) Gene ontology (GO) enrichment analysis of differential gene expression between the two groups of chondrocytes. GO enrichment analysis was performed on each of the three GO categories (BP, MF, and CC). (For interpretation of the references to colour in this figure legend, the reader is referred to the Web version of this article.)

3. Discussion

In this study, we explored the mechanisms underlying IL-1β-induced inflammation, and investigated the effect of PRP on TMJ condylar chondrocytes. The data collected suggest that IL-1β causes inflammation and apoptosis of TMJ condylar chondrocytes through the classical NF-κB and TNF signaling pathways. PRP mitigates IL-1β-induced damage to chondrocytes, mainly by acting on the cell cycle, promoting DNA replication, and upregulating the PI3K-AKT and MAPK signaling pathways to increase proliferation and

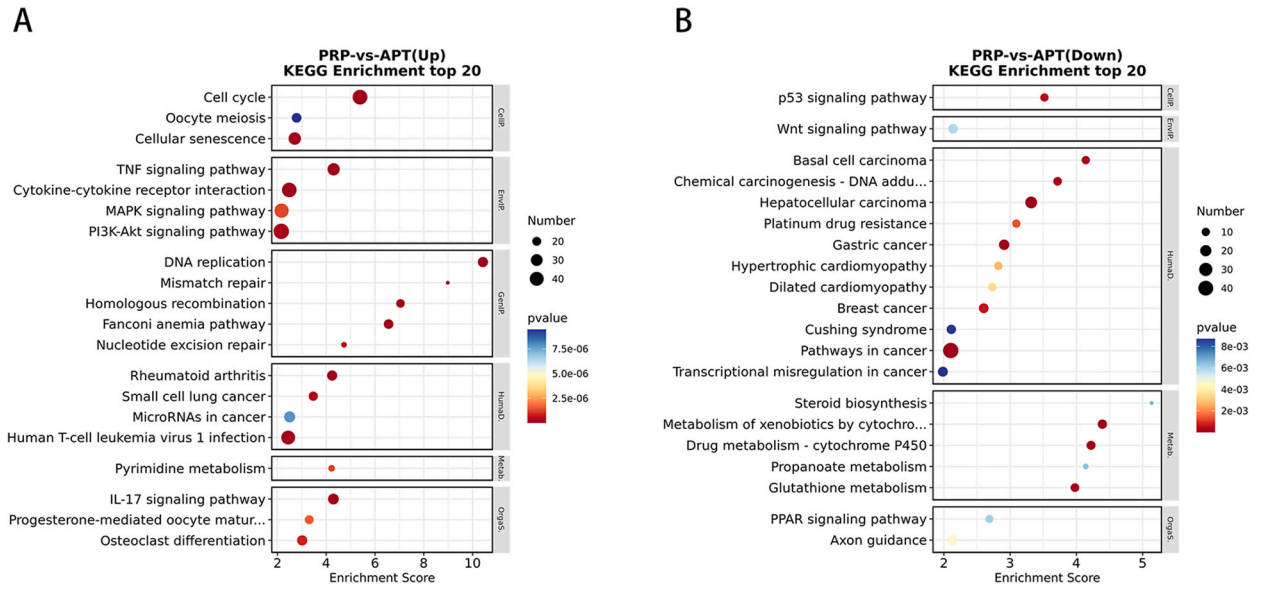

Fig. 6. Kyoto Encyclopedia of Genes and Genomes (KEGG) pathway analysis of differentially expressed genes (DEGs) in the two groups of treated chondrocytes. (A) KEGG pathway analysis of upregulated DEGs in IL-1β-induced inflammatory chondrocytes treated with PRP. (B) KEGG pathway analysis of downregulated DEGs in IL-1β-induced inflammatory chondrocytes treated with PRP.

inhibit apoptosis. Furthermore, we found that PRP induces inflammation in chondrocytes.

The results of this study indicate that IL-1β-induced chondrocyte inflammation is related to inflammatory function and pathway activation, including the inflammatory response as well as the TNF, NF-κB, IL-17, chemokine, and NOD-like receptor signaling pathways. Signaling cascades related to cell cycle regulation, proliferation, and inhibition of apoptosis (i.e., the FoxO, Apelin, MAPK, and PI3K/Akt signaling pathways) were downregulated. The expression of inflammation-related factors such as *IL-17b*, *IL-6*, *Tnfaip2*, *Tnfaip3*, and *Enpp2*, and that of matrix catabolism-related genes (i.e., *Mmp3* and *Mmp9*) was increased. Simultaneously, the expression of the anti-apoptotic gene *Plk3* and that of *Nr4a1* and *Sfrp1*, which have *anti*-TMJ-OA effects, was decreased. The overexpression of a series of inflammation-related mRNA in chondrocytes, such as *IL-17b*, *IL-6*, *IL-7*, *Tnfaip2*, and *Tnfaip3*, partially overlapped with the results of a study targeting mRNA in the synovial fluid of patients with TMJ-OA [7]. A previous study using Western blotting found that *Mmp3* and *Mmp9* levels in the joint fluid of patients with TMJ-OA were significantly elevated compared to healthy individuals [27]. This is consistent with the present study, in which there is a strong correlation between mRNA overexpression of the degradation enzymes *Mmp3* and *Mmp9* and OA activity. Synovitis is closely related to TMJ-OA. From our results, it can be inferred that IL-1β released by synovial tissue stimulates the articular cartilage to synthesize inflammatory mediators such as IL-17, IL-6, MMP3, and MMP9. These inflammatory mediators are secreted into the synovial fluid and induce the synovial tissue to produce more inflammatory mediators, ultimately inducing a cascade amplification of inflammation that leads to TMJ-OA. In agreement with the results of this study, Pang et al. conducted transcriptome analysis on IL-1β-induced mouse knee joint chondrocytes, and reported the involvement of the TNF, NOD-like receptor, NF-κB, and IL-17 signaling pathways [28]. It is worth noting that, unlike the condyles of most joints such as the knee and hip, which are mainly composed of hyaline cartilage [29], the TMJ condyle is a fibrocartilage tissue [30]. The mRNA expression pattern of fibrochondrocytes stimulated by IL-1β differs from that observed in hyaline chondrocytes, which distinguishes our findings from those of previous studies.

Compared with the inflammatory chondrocytes induced by IL-1β alone, the addition of PRP upregulated the TNF and IL-17 signaling pathways, related to inflammation. The expression of the inflammation-related factor *Il17b* was decreased; however, the expression of *Il6*, *Tnfaip2*, *Tnfaip3*, and *Enpp2* was increased, as was that of matrix catabolism-related *Mmp3* and *Mmp9*. In contrast with the findings from previous research on human chondrocytes [31] stating that PRP can reduce the IL-1β-induced inflammatory response of chondrocytes and increase matrix synthesis and metabolism, this study found that PRP promoted an inflammatory response and matrix decomposition in chondrocytes. This may be related to the fact that PRP itself contains pro-inflammatory factors such as IL-1β and IL-6 [32], and that the inflammatory environment induced by IL-1β can cause PRP to release IL-1β, IL-6, IL-8, and TNF-α [33]. The promoting effect on inflammation and the activation of the TNF and IL-17 signaling pathways, as well as the increase in catabolism (increased expression of the *Mmp3*, *Mmp9*, and *Mmp13* genes), are highly likely to be related to this. It is worth exploring how to minimize or remove pro-inflammatory factors during PRP manufacture. Previous studies have shown that the presence and production of pro-inflammatory factors are positively correlated with white blood cell content [31,32].

However, after PRP treatment, the MAPK and PI3K-AKT signaling pathways related to cell cycle regulation, proliferation, and apoptosis inhibition were upregulated. Genes involved in DNA replication, cell cycle, and nucleotide exclusion repair processes were also significantly enriched. The proliferation-related gene *Mki67* was overexpressed, and the expression of genes related to DNA replication and damage repair, such as *Top2a, Ect2, Rrm2,* and *Anln,* was increased in this study. The MAPK signaling pathway plays an

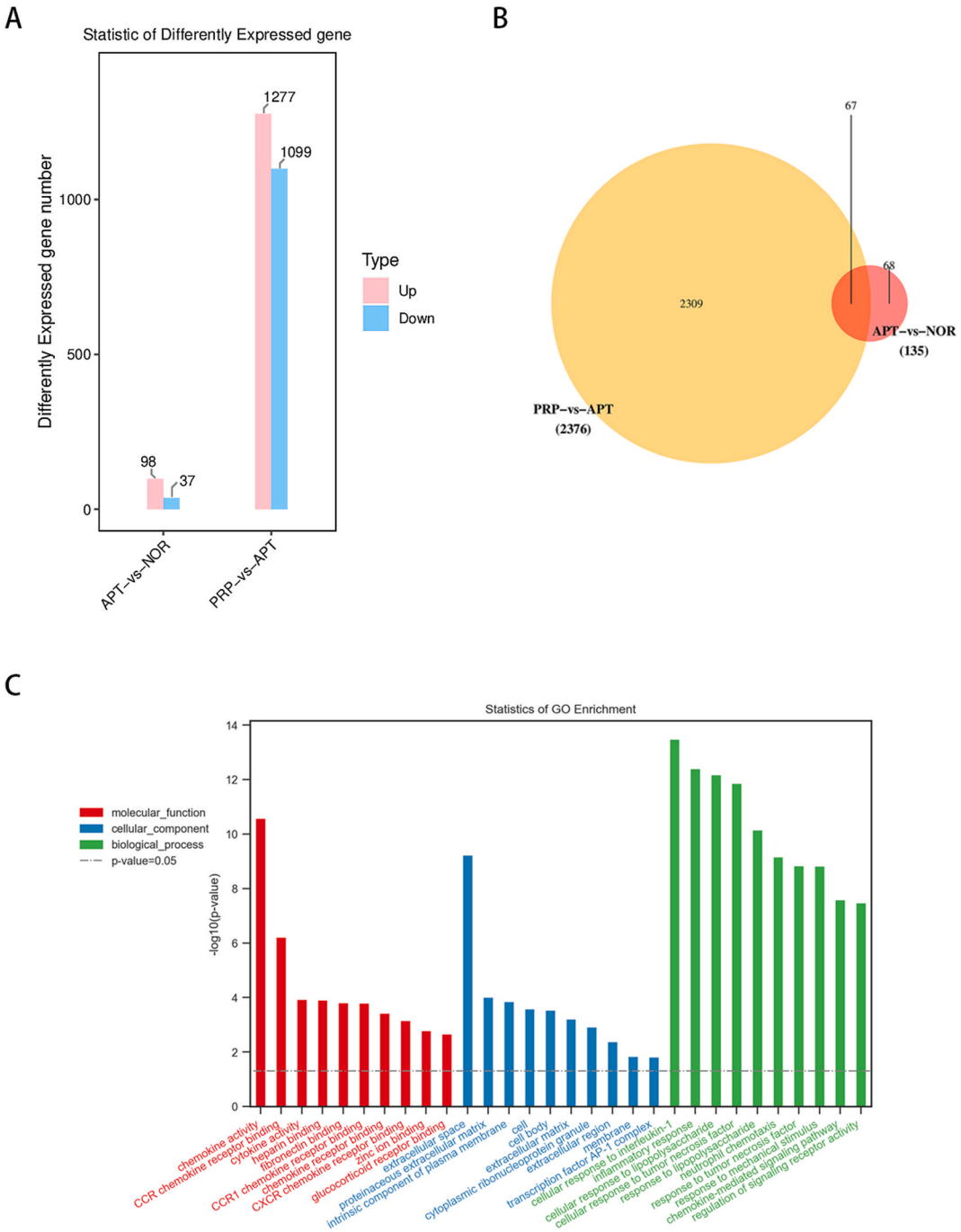

Fig. 7. Platelet-rich plasma (PRP)- vs. interleukin (IL)-1β-induced differential gene expression on inflammatory chondrocytes. (A) Up/downregulation of two sets of differentially expressed genes (DEGs). (B) Overlap between the two sets of DEGs. (C) Gene ontology (GO) analysis of overlapping genes.

important role in the regulation of proliferation in mammalian cells, in a manner inextricable from other signal transduction systems due to shared substrates and cross-cascade interactions [34]. In the MAPK family, the ERK1/2 signaling pathway is key in determining cell fate in response to external stimuli, mainly by promoting proliferation and regulating terminal cell differentiation [35]. The PI3K-AKT pathway is essential for cartilage homeostasis, and compared with normal cartilage, it is downregulated in human cartilage tissue with OA [36,37]. The PI3K-AKT signaling pathway is a vital regulator of cell survival and apoptosis [38], and reduced activity of this pathway was found in OA-like chondrocytes exposed to IL-1β or TNF-α, as reported in previous studies [39,40]. However, the role of PI3K/AKT in inflammatory responses is not yet fully understood. NF-κB is the main regulatory factor of OA-related inflammatory

Table 1
Primer sequences in qRT-PCR.

Primer name	Primer sequence (5′-3′)
GAPDH	F: GCCTTCTTGGGACTGATGTTGTTG
	R: GTCTGTTGTGGGTGGTATCCTCTG
Il6	F: GTGGTGTCGCAGGAGGAGTTG
	R: CGTGTGATTGCTAGTGCCGTTG
Tnfaip2	F: CACGGACTCCAGCAGACAGAAC
	R: CTTTCCCAGAGGCGGTGACAG
Tnfaip3	F: GGACCCTGAGACCTTACCAATGTG
	R: AGATTTTCGCCAAAAGTGCCTGTC
Mmp3	F: ACCGCCAACTATGACCAGGATAAG
	R: TGCTTGCCCAGGAAGACGAAG
Mmp9	F: CCACCTCCAACCTTCTTCTCCTTC
	R: AAGCGGCTGGCACGGAATAG
Nr4a1	F: GAGACCTACAGCACCGCCATATC
	R: CCAGGGACTTTCGGCTACAGAG
Plk3	F: ATGGCAGAGGTGAAGCAGCAG
	R: CGAAGAGCGAGCAGAGGAAGAC
Enpp2	F: TGCTCTTCCTTCTTGCCATCTCC
	R: TCCCTTGCCCCTTCCTTTTGC
Il17b	F: TCCGCCCTCCGTTAATCATCTTC
	R: CAGGACCGCAGTTTCTCAATGTTG

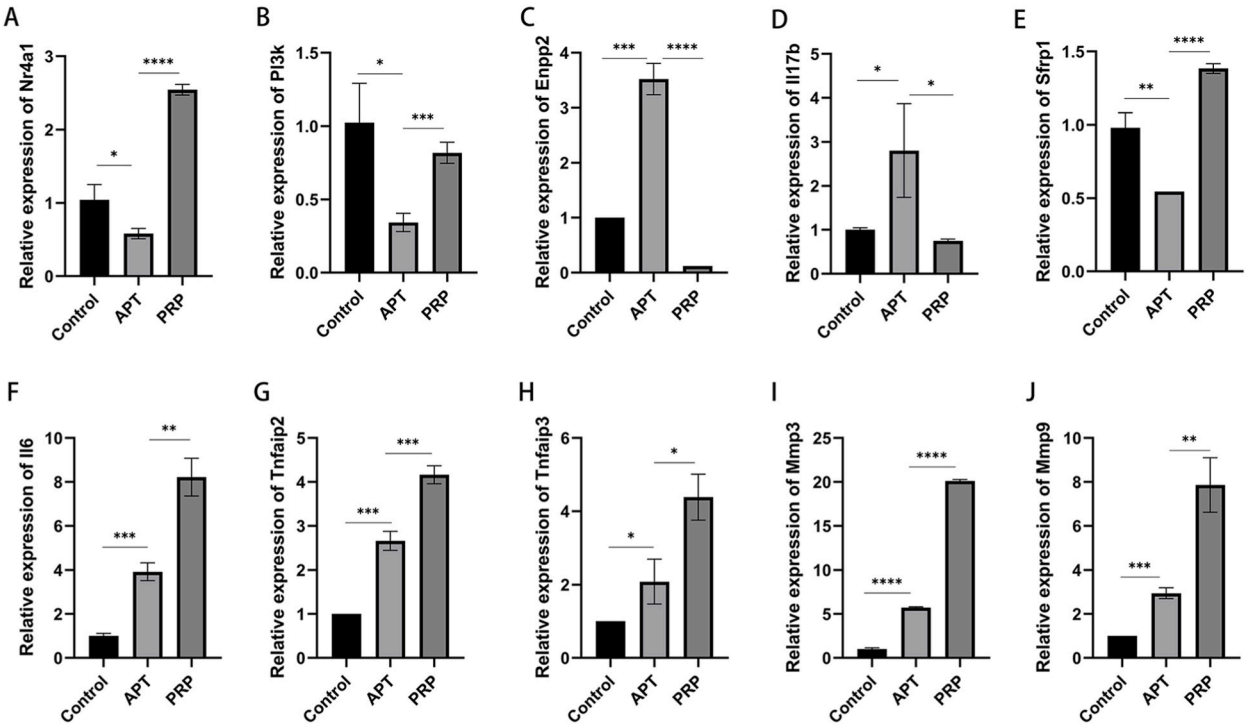

Fig. 8. The effect of interleukin (IL)-1β and platelet-rich plasma (PRP) on the mRNA expression of osteoarthritis-related genes. (A) *Nr4a1*, (B) *Plk3*, (C) *Enpp2*, (D) *IL-17b*, (E) *Sfrp1*, (F) *IL-6*, (G) *Tnfaip2*, (H)*Tnfaip3*, (I) *Mmp3*, (J) *Mmp9*. Data are presented as mean ± S.D. (n = 3). *p < 0.05; **p < 0.01; ***p < 0.001; ****p < 0.0001.

mediators, mainly influenced by IκB kinase-mediated IκBα degradation and activation of p65/RelA phosphorylation [41]. PKA/AKT can influence NF-κB activity by engaging IκB kinase [42]. Therefore, active PI3K and AKT participate in NF-κB p65 phosphorylation and nuclear translocation, thereby promoting the production of inflammatory mediators. In this study, PI3K/AKT was inhibited in IL-1β-induced inflammatory condylar chondrocytes, which contradicts previous research results stating that IL-1β promotes PI3K/AKT pathway expression in chondrocytes [43,44]. This may be explained by different chondrocyte sources between studies. Interestingly, the P53 signaling pathway, which induces cell cycle arrest, senescence, and apoptosis, was downregulated. Simultaneously, the expression of the anti-apoptotic genes *Plk3*, *Bcl2a1*, and *Bok* was increased, and that of *Nr4a1* and *Sfrp1* with *anti*-OA effects was also increased. Furthermore, it is possible to regulate the cell cycle, promote cell proliferation, and inhibit apoptosis through the MAPK and

PI3K/AKT signaling pathways. Owing to the abundance of various cytokines induced by PRP, the actual mechanism may involve cytokine-cytokine receptor interactions.

After activation, platelets in PRP undergo degranulation, releasing substantial amounts of biologically active growth factors (GFs) that promote tissue repair [45]. This includes platelet-derived growth factor, transforming growth factor-β 1, transforming growth factor-β 2, insulin-like growth factor 1, vascular endothelial growth factor, and epidermal growth factor [46]. Based on previous research, the binding of GFs to receptors in the membrane of surrounding cells involved in repair has been speculated to control the metabolic function of chondrocytes and subchondral bone, maintaining a steady state between protein polysaccharide synthesis and degradation, which is beneficial for the stability of chondrocytes [47]. Meanwhile, signals from the GFs are transmitted to the nucleus through a signaling pathway to stimulate cell proliferation and differentiation, leading to the formation of new cartilage [48]. For example, IGF-1 is a strong activator of AKT phosphorylation, which activates AKT to promote collagen II synthesis. Moreover, IGF-1 influences IL-1β-induced NF-κB activation in human chondrocytes, exerting inhibitory effects on a process closely related to cartilage degradation [37]. Taking into consideration the cytokine-rich composition of PRP and the intricate web of interactions among various pathways, the precise mechanisms of its action warrant further exploration.

Clinical studies have found that the injection of PRP directly into the inferior space of the TMJ in contact with the condylar cartilage not only effectively alleviate symptoms but can also help repair the condylar bone, as confirmed via cone beam computed tomography [19,49]. However, the specific mechanism underlying the effectiveness of the treatment has not yet been elucidated. This study suggests that elucidating the mechanism underlying the effect of PRP treatment on TMJ-OA is a promising research direction for future studies. PRP acts specifically on chondrocytes, and may exert therapeutic effects by regulating the cell cycle, promoting proliferation, or inhibiting apoptosis.

This study has some limitations. The first is the complex composition of PRP. In addition to GFs, a large number of microRNAs carried by exosomes may be involved in post-transcriptional regulation [50]. Second, this study is limited to the transcriptome. In future research, we intend to study subsequent phases in the protein expression process such as post-transcriptional regulation and translation through microRNA sequencing and proteomics, to provide a more comprehensive understanding of the intricate mechanisms involved in the effect of PRP. Furthermore, a potential avenue for future research involves optimizing the purification of PRP components, thereby enhancing its therapeutic efficacy against OA.

4. Conclusions

The protective effect of PRP on IL-1β-induced chondrocyte injury is primarily achieved by activation of the MAPK and PI3K/AKT signaling pathways, increasing cell proliferation and inhibiting cell apoptosis. Notably, PRP promotes inflammation and matrix catabolism.

5. Materials and methods

5.1. Extraction and identification of TMJ condylar chondrocytes

Four-week-old female Sprague-Dawley rats were euthanized under anesthesia (5% pentobarbital sodium by intraperitoneal injection at a dose of 5 mL/kg body weight). The condylar cartilage of the TMJ was dissected and collected under sterile conditions, and the tissue was treated with 2 mg/mL (0.1%) collagenase II at 37 °C for 4 h. The digested cartilage tissue was resuspended, filtered through an 80-mesh cell sieve, and seeded into a tissue culture bottle. Chondrocytes were grown in high-glucose Dulbecco's Modified Eagle Medium containing 10% fetal bovine serum and 1% penicillin/streptomycin. The obtained chondrocytes were cultured at 37 °C in a constant temperature incubator with 5% CO_2, and the culture medium was changed after 24 h. When the adherent cells covered 80%–90% of the flask wall, they were digested and harvested using 0.25% trypsin EDTA (Beyotime, Shanghai, China) for subculture. This study used 3rd to 5th generation chondrocytes. Successful in vitro culture of condylar chondrocytes was confirmed using inverted phase contrast microscopy, TB staining, collagen II immunohistochemical staining, and fluorescent staining.

5.1.1. Induction of chondrocyte inflammation in vitro

The CCK-8 (Beyotime, Shanghai, China) method was used to evaluate the effect of different concentrations of IL-1β on the viability of chondrocytes. Chondrocytes were seeded in 96-well plates at a density of 5×10^3 cells/well. After cell adhesion, IL-1β (5, 10, and 20 ng/mL) was used to treat cultured cells for 6, 12, 24, 48, and 72 h. The concentration and duration of action of IL-1β were based on the results of the CCK-8 experiment.

5.1.2. Preparation and concentration standardization of PRP

Whole blood samples were collected from 8-week-old healthy rats, and 2.5% sodium citrate anticoagulant was added at a ratio of 1:10. After centrifuging at 160 *g* for 10 min, the platelet-containing plasma was carefully collected and transferred to a new centrifuge tube, followed by centrifugation at 250*g* for 15 min. The supernatant was discarded, and the platelet particles were resuspended in the residual plasma to obtain PRP. The BCA Protein Assay Kit (Beyotime, Shanghai, China) was used for protein concentration assessment and further standardization of the PRP. The protein concentrations used in the experiment were 50 and 500 μg/mL.

5.1.3. Grouping, treatment, and RNA extraction from chondrocytes

Chondrocytes were seeded into 96-well plates at a density of 5×10^3 cells/well. After normal cultivation for 24 h and cell adhesion,

PBS, 10 ng/mL IL-1β or 10 ng/mL IL-1β + 500 μg/mL PRP were added. Cell viability was measured using the CCK-8 method at 6, 12, 24, 48, and 72 h. Chondrocytes with an appropriate growth status were seeded into a 6-well plate at a density of 2×10^4 cells/well. After the cells covered 80% of the well surface, PBS, 10 ng/mL IL-1β or 10 ng/mL IL-1β + 500 μg/mL PRP were added for 24 h. RNAiso Plus (TAKARA, Shiga, Japan) was used for subsequent RNA extractions. Each RNA sample was dissolved in 10 μL of DEPC H_2O and stored at −80 °C until further use.

5.1.4. Transcriptome sequencing

After the total RNA was extracted and digested with DNase, mRNA was enriched with magnetic beads containing oligo (dT). Interrupting reagents were used to break mRNA into short fragments. The interrupted mRNA was used as a template, and first-strand cDNA was synthesized using six random base primers. A two-strand reaction system was prepared to synthesize second-strand cDNA, which was purified using a PureLink® RNA Mini Kit (12183025, Invitrogen, Carlsbad, CA, USA). Purified double-stranded cDNA was subjected to end repair, poly A-tailed addition, and sequencing connections, followed by fragment size selection. Finally, PCR amplification was performed. After quality inspection with an Agilent 2100 Bioanalyzer, the constructed library was sequenced using an Illumina HiSeq 2500 sequencer (Illumina, USA) to generate 125 bp of double-ended data.

5.1.5. Bioinformatics analysis

Raw image data files obtained from high-throughput sequencing were transformed into raw sequencing sequences, known as RawData or RawReads, through base-calling analysis. The results were stored in the FASTQ (fq) file format, which contained information of sequences (reads) and their corresponding quality information. A large amount of double-ended sequencing data was obtained using the Illumina platform.

Considering the impact of the data error rate on the results, the fastp [51] software was used to pre-process the original data, and the number of reads in the entire quality control process was statistically summarized. Hisat2 was used [52] to perform sequence alignment between CleanReads and the designated reference genome to obtain position information as well as sequence feature information unique to the sequencing samples. Known reference gene sequences and annotation files were used to assess the abundance of each protein-coding gene per sample through sequence similarity alignment. The htseq-count software [53] was used to obtain the number of reads aligned to the protein-coding genes in each sample. The expression levels of the protein-coding genes were calculated using the FPKM [54] method (i.e., fragments per kilobase per million reads). DESeq2 software [55] was used to standardize the number of counts for each sample gene (using BaseMean values to estimate expression levels) and calculate multiple differences. A negative binomial distribution test (NB) was used to evaluate the significance of identified differences, and finally, the differential protein-coding genes were screened according to the difference multiple and difference significance test results. After identifying the DEGs, functional GO and KEGG pathway analyses were performed.

5.1.6. qRT-PCR assay

Based on the sequencing results, 10 DEGs related to OA were selected for qRT-PCR validation. RNA production and purity were measured using a NanoDrop 1000 spectrophotometer (Thermo Fisher Scientific, Waltham, MA, USA). cDNA synthesis was performed using the ReverTra Ace qPCR RT Master Mix with gDNA Remover (Code No. FSQ-301, TOYOBO, Osaka, Japan). THUNDERBIRD ® Next SYBR ® QPCR Mix (Code No. QPX-201T, TOYOBO) was used for the qRT-PCR quantification and analysis. The thermocycler protocol was as follows: 95 °C for 30 s, 40 cycles at 95 °C for 15 s, and 60 °C for 30 s (using LightCycler®480II [Idaho Technology Inc. and Roche Diagnostic Systems, Basel, Switzerland] to perform qRT-PCR and data acquisition).

Ethical approval statement

The animal study protocol was approved by the Institutional Review Board (or Ethics Committee) of the Ninth People's Hospital affiliated with the Shanghai Jiao Tong University School of Medicine (SH9H-2022-A880-1, 2022/09/19). The requirement for informed consent was not applicable in this study.

Funding

This research was funded by the Fundamental Research Funds for the Central Universities, grant/award number YG2022QN062; the Fundamental Research Program funding of Ninth People's Hospital affiliated with Shanghai Jiao Tong University School of Medicine, grant/award number JYZZ133; the Scientific Research Project of the Shanghai Municipal Health Commission, grant/award number 20214Y0447; the Shanghai Municipal Health Commission Supporting Discipline Construction Project, 2023ZDFC0303 and the Scientific Research Program of Shanghai Rehabilitation Clinical Medical Research Center, grant/award number 21MC1930200.

Data availability statement

The data associated with this study has not been deposited into a public repository. However, it will be made available on request.

CRediT authorship contribution statement

Shasha Liu: Writing – review & editing, Writing – original draft, Visualization, Validation, Supervision, Software, Resources,

Project administration, Methodology, Investigation, Funding acquisition, Formal analysis, Data curation, Conceptualization. **Chaolun Wu:** Visualization, Validation, Project administration, Investigation. **Yuxin Zhang:** Writing – original draft, Validation, Investigation, Formal analysis.

Declaration of competing interest

The authors declare that they have no known competing financial interests or personal relationships that could have appeared to influence the work reported in this paper.

Acknowledgements

We would like to thank the North Central Laboratory of Shanghai Ninth People's Hospital for providing the conditions for cell culture and subsequent experiments.

References

[1] A. Whyte, R. Boeddinghaus, A. Bartley, R. Vijeyaendra, Imaging of the temporomandibular joint, Clin. Radiol. 76 (2021) 76, https://doi.org/10.1016/j.crad.2020.06.020, e21–76.e35.
[2] S.S. Liu, L.L. Xu, S.J. Lu, M.Y. Mao, L.K. Liu, B. Cai, Diagnostic performance of magnetic resonance imaging for degenerative temporomandibular joint disease, J. Oral Rehabil. 50 (2023) 24–30, https://doi.org/10.1111/joor.13386.
[3] K. Kim, A. Wojczyńska, J.Y. Lee, The incidence of osteoarthritic change on computed tomography of Korean temporomandibular disorder patients diagnosed by RDC/TMD; a retrospective study, Acta Odontol. Scand. 74 (2016) 337–342, https://doi.org/10.3109/00016357.2015.1136678.
[4] L.L.Q. Pantoja, I.P. de Toledo, Y.M. Pupo, A.L. Porporatti, G. De Luca Canto, L.F. Zwir, E.N.S. Guerra, Prevalence of degenerative joint disease of the temporomandibular joint: a systematic review, Clin. Oral Invest. 23 (2019) 2475–2488, https://doi.org/10.1007/s00784-018-2664-y.
[5] S.N. Delpachitra, G. Dimitroulis, Osteoarthritis of the temporomandibular joint: a review of aetiology and pathogenesis, Br. J. Oral Maxillofac. Surg. 60 (2022) 387–396, https://doi.org/10.1016/j.bjoms.2021.06.017.
[6] C. Cui, L. Zheng, Y. Fan, J. Zhang, R. Xu, J. Xie, X. Zhou, Parathyroid hormone ameliorates temporomandibular joint osteoarthritic-like changes related to age, Cell Prolif. 53 (2020) e12755, https://doi.org/10.1111/cpr.12755.
[7] R. Vernal, E. Velasquez, J. Gamonal, J.A. Garcia-Sanz, A. Silva, M. Sanz, Expression of pro-inflammatory cytokines in osteoarthritis of the temporomandibular joint, Arch. Oral Biol. 53 (2008) 910–915, https://doi.org/10.1016/j.archoralbio.2008.04.004.
[8] X.D. Wang, S.J. Cui, Y. Liu, Q. Luo, R.J. Du, X.X. Kou, J.N. Zhang, Y.H. Zhou, Y.H. Gan, Deterioration of mechanical properties of discs in chronically inflamed TMJ, J. Dent. Res. 93 (2014) 1170–1176, https://doi.org/10.1177/0022034514552825.
[9] L. Liao, S. Zhang, G.Q. Zhou, L. Ye, J. Huang, L. Zhao, D. Chen, Deletion of Runx2 in condylar chondrocytes disrupts TMJ tissue homeostasis, J. Cell. Physiol. 234 (2019) 3436–3444, https://doi.org/10.1002/jcp.26761.
[10] J. Deschner, B. Rath-Deschner, S. Agarwal, Regulation of matrix metalloproteinase expression by dynamic tensile strain in rat fibrochondrocytes, Osteoarthritis Cartilage 14 (2006) 264–272, https://doi.org/10.1016/j.joca.2005.09.005.
[11] E.A. Al-Moraissi, L.M. Wolford, E. Ellis, A. Neff, The hierarchy of different treatments for arthrogenous temporomandibular disorders: a network meta-analysis of randomized clinical trials, J. Cranio-Maxillo-Fac. Surg. 48 (2020) 9–23, https://doi.org/10.1016/j.jcms.2019.10.004.
[12] Z. Peng, H. Sun, V. Bunpetch, Y. Koh, Y. Wen, D. Wu, H. Ouyang, The regulation of cartilage extracellular matrix homeostasis in joint cartilage degeneration and regeneration, Biomaterials 268 (2021) 120555, https://doi.org/10.1016/j.biomaterials.2020.120555.
[13] Z. Huang, M. Zhou, Q. Wang, M. Zhu, S. Chen, H. Li, Mechanical and hypoxia stress can cause chondrocytes apoptosis through over-activation of endoplasmic reticulum stress, Arch. Oral Biol. 84 (2017) 125–132, https://doi.org/10.1016/j.archoralbio.2017.09.021.
[14] K. Lu, F. Ma, D. Yi, H. Yu, L. Tong, D. Chen, Molecular signaling in temporomandibular joint osteoarthritis, J Orthop Translat 32 (2022) 21–27, https://doi.org/10.1016/j.jot.2021.07.001.
[15] T.E. Foster, B.L. Puskas, B.R. Mandelbaum, M.B. Gerhardt, S.A. Rodeo, Platelet-rich plasma: from basic science to clinical applications, Am. J. Sports Med. 37 (2009) 2259–2272, https://doi.org/10.1177/0363546509349921.
[16] W.S. Pietrzak, B.L. Eppley, Platelet rich plasma: biology and new technology, J. Craniofac. Surg. 16 (2005) 1043–1054, https://doi.org/10.1097/01.scs.0000186454.07097.bf.
[17] L. Shen, T. Yuan, S. Chen, X. Xie, C. Zhang, The temporal effect of platelet-rich plasma on pain and physical function in the treatment of knee osteoarthritis: systematic review and meta-analysis of randomized controlled trials, J. Orthop. Surg. Res. 12 (2017) 16, https://doi.org/10.1186/s13018-017-0521-3.
[18] Y. Huang, X. Liu, X. Xu, J. Liu, Intra-articular injections of platelet-rich plasma, hyaluronic acid or corticosteroids for knee osteoarthritis: a prospective randomized controlled study, Orthopä 48 (2019) 239–247, https://doi.org/10.1007/s00132-018-03659-5.
[19] S.S. Liu, L.L. Xu, S. Fan, S.J. Lu, L. Jin, L.K. Liu, Y. Yao, B. Cai, Effect of platelet-rich plasma injection combined with individualised comprehensive physical therapy on temporomandibular joint osteoarthritis: a prospective cohort study, J. Oral Rehabil. 49 (2022) 150–159, https://doi.org/10.1111/joor.13261.
[20] S. Cömert Kiliç, M. Güngörmüş, M.A. Sümbüllü, Is arthrocentesis plus platelet-rich plasma superior to arthrocentesis alone in the treatment of temporomandibular joint osteoarthritis? A randomized clinical trial, J. Oral Maxillofac. Surg. 73 (2015) 1473–1483, https://doi.org/10.1016/j.joms.2015.02.026.
[21] C.B. Wu, N.N. Sun, D. Zhang, Q. Wang, Q. Zhou, Efficacy analysis of splint combined with platelet-rich plasma in the treatment of temporomandibular joint osteoarthritis, Front. Pharmacol. 13 (2022) 996668, https://doi.org/10.3389/fphar.2022.996668.
[22] C. Haddad, A. Zoghbi, E. El Skaff, J. Touma, Platelet-rich plasma injections for the treatment of temporomandibular joint disorders: a systematic review, J. Oral Rehabil. 50 (2023) 1330–1339, https://doi.org/10.1111/joor.13545.
[23] R. Asjid, T. Faisal, K. Qamar, S.A. Khan, A. Khalil, M.S. Zia, Platelet-rich plasma-induced inhibition of chondrocyte apoptosis directly affects cartilage thickness in osteoarthritis, Cureus 11 (2019) e6050, https://doi.org/10.7759/cureus.6050.
[24] X.P. Ge, Y.H. Gan, C.G. Zhang, C.Y. Zhou, K.T. Ma, J.H. Meng, X.C. Ma, Requirement of the NF-κB pathway for induction of Wnt-5A by interleukin-1β in condylar chondrocytes of the temporomandibular joint: functional crosstalk between the Wnt-5A and NF-κB signaling pathways, Osteoarthritis Cartilage 19 (2011) 111–117, https://doi.org/10.1016/j.joca.2010.10.016.
[25] H. Tabeian, B.F. Betti, C. Dos Santos Cirqueira, T.J. de Vries, F. Lobbezoo, A.V. Ter Linde, B. Zandieh-Doulabi, M.I. Koenders, V. Everts, A.D. Bakker, IL-1β damages fibrocartilage and upregulates MMP-13 expression in fibrochondrocytes in the condyle of the temporomandibular joint, Int. J. Mol. Sci. 20 (2019) 2260, https://doi.org/10.3390/ijms20092260.
[26] C. Zhang, P. Wang, P. Jiang, Y. Lv, C. Dong, X. Dai, L. Tan, Z. Wang, Upregulation of lncRNA HOTAIR contributes to IL-1β-induced MMP overexpression and chondrocytes apoptosis in temporomandibular joint osteoarthritis, Gene 586 (2016) 248–253, https://doi.org/10.1016/j.gene.2016.04.016.
[27] M. Kanyama, T. Kuboki, S. Kojima, T. Fujisawa, T. Hattori, M. Takigawa, A. Yamashita, Matrix metalloproteinases and tissue inhibitors of metalloproteinases in synovial fluids of patients with temporomandibular joint osteoarthritis, J. Orofac. Pain 14 (2000) 20–30.
[28] Y. Pang, L. Zhao, X. Ji, K. Guo, X. Yin, Analyses of transcriptomics upon IL-1β-stimulated mouse chondrocytes and the protective effect of catalpol through the NOD2/NF-κB/MAPK signaling pathway, Molecules 28 (2023) 1606, https://doi.org/10.3390/molecules28041606.

[29] A.J. Sophia Fox, A. Bedi, S.A. Rodeo, The basic science of articular cartilage: structure, composition, and function, Sport Health 1 (2009) 461–468, https://doi.org/10.1177/1941738109350438.
[30] M.C. Embree, M. Chen, S. Pylawka, D. Kong, G.M. Iwaoka, I. Kalajzic, H. Yao, C. Shi, D. Sun, T.J. Sheu, D.A. Koslovsky, A. Koch, J.J. Mao, Exploiting endogenous fibrocartilage stem cells to regenerate cartilage and repair joint injury, Nat Commn 7 (2016) 13073, https://doi.org/10.1038/ncomms13073.
[31] G.M. van Buul, W.L.M. Koevoet, N. Kops, P.K. Bos, J.A.N. Verhaar, H. Weinans, M.R. Bernsen, G.J.V.M. van Osch, Platelet-rich plasma releasate inhibits inflammatory processes in osteoarthritic chondrocytes, Am. J. Sports Med. 39 (2011) 2362–2370, https://doi.org/10.1177/0363546511419278.
[32] H. Masuki, T. Okudera, T. Watanebe, M. Suzuki, K. Nishiyama, H. Okudera, K. Nakata, K. Uematsu, C.Y. Su, T. Kawase, Growth factor and pro-inflammatory cytokine contents in platelet-rich plasma (PRP), plasma rich in growth factors (PRGF), advanced platelet-rich fibrin (A-PRF), and concentrated growth factors (CGF), Int. J. Implant Dent. 2 (2016) 19, https://doi.org/10.1186/s40729-016-0052-4.
[33] E. Anitua, M. Zalduendo, M. Troya, S. Padilla, G. Orive, Leukocyte inclusion within a platelet rich plasma-derived fibrin scaffold stimulates a more pro-inflammatory environment and alters fibrin properties, PLoS One 10 (2015) e0121713, https://doi.org/10.1371/journal.pone.0121713.
[34] W. Zhang, H.T. Liu, MAPK signal pathways in the regulation of cell proliferation in mammalian cells, Cell Res. 12 (2002) 9–18, https://doi.org/10.1038/sj.cr.7290105.
[35] I. Prasadam, T. Friis, W. Shi, S. van Gennip, R. Crawford, Y. Xiao, Osteoarthritic cartilage chondrocytes alter subchondral bone osteoblast differentiation via MAPK signalling pathway involving ERK1/2, Bone 46 (2010) 226–235, https://doi.org/10.1016/j.bone.2009.10.014.
[36] K.M. Fisch, R. Gamini, O. Alvarez-Garcia, R. Akagi, M. Saito, Y. Muramatsu, T. Sasho, J.A. Koziol, A.I. Su, M.K. Lotz, Identification of transcription factors responsible for dysregulated networks in human osteoarthritis cartilage by global gene expression analysis, Osteoarthritis Cartilage 26 (2018) 1531–1538, https://doi.org/10.1016/j.joca.2018.07.012.
[37] K. Sun, J. Luo, J. Guo, X. Yao, X. Jing, F. Guo, The PI3K/AKT/mTOR signaling pathway in osteoarthritis: a narrative review, Osteoarthritis Cartilage 28 (2020) 400–409, https://doi.org/10.1016/j.joca.2020.02.027.
[38] S.C. Rosa, A.T. Rufino, F. Judas, C. Tenreiro, M.C. Lopes, A.F. Mendes, Expression and function of the insulin receptor in normal and osteoarthritic human chondrocytes: modulation of anabolic gene expression, glucose transport and GLUT-1 content by insulin, Osteoarthritis Cartilage 19 (2011) 719–727, https://doi.org/10.1016/j.joca.2011.02.004.
[39] I. Stanic, A. Facchini, R.M. Borzì, R. Vitellozzi, C. Stefanelli, M.B. Goldring, C. Guarnieri, A. Facchini, F. Flamigni, Polyamine depletion inhibits apoptosis following blocking of survival pathways in human chondrocytes stimulated by tumor necrosis factor-alpha, J. Cell. Physiol. 206 (2006) 138–146, https://doi.org/10.1002/jcp.20446.
[40] X. Yao, J. Zhang, X. Jing, Y. Ye, J. Guo, K. Sun, F. Guo, Fibroblast growth factor 18 exerts anti-osteoarthritic effects through PI3K-AKT signaling and mitochondrial fusion and fission, Pharmacol. Res. 139 (2019) 314–324, https://doi.org/10.1016/j.phrs.2018.09.026.
[41] M.C. Choi, J. Jo, J. Park, H.K. Kang, Y. Park, NF-κB signaling pathways in osteoarthritic cartilage destruction, Cells 8 (2019), https://doi.org/10.3390/cells8070734.
[42] S. Balwani, R. Chaudhuri, D. Nandi, P. Jaisankar, A. Agrawal, B. Ghosh, Regulation of NF-ɨB activation through a novel PI-3K-independent and PKA/Akt-dependent pathway in human umbilical vein endothelial cells, PLoS One 7 (2012) e46528, https://doi.org/10.1371/journal.pone.0046528.
[43] M. Kapoor, J. Martel-Pelletier, D. Lajeunesse, J.P. Pelletier, H. Fahmi, Role of pro-inflammatory cytokines in the pathophysiology of osteoarthritis, Nat. Rev. Rheumatol. 7 (2011) 33–42, https://doi.org/10.1038/nrrheum.2010.196.
[44] C. Park, J.W. Jeong, D.S. Lee, M.J. Yim, J. M Lee, M.H. Han, S. Kim, H.S. Kim, G.Y. Kim, E.K. Park, et al., Sargassum serratifolium extract attenuates interleukin-1-induced oxidative stress and inflammatory response in chondrocytes by suppressing the activation of NF- κB, p38 MAPK, and PI3K/Akt, Int. J. Mol. Sci. 19 (2018) 2308, https://doi.org/10.3390/ijms19082308.
[45] K.M. Lacci, A. Dardik, Platelet-rich plasma- support for its use in wound healing, Yale J. Biol. Med. 83 (2010), 1–9.
[46] P. Everts, K. Onishi, P. Jayaram, J.F. Lana, K. Mautner, Platelet-rich plasma: new performance understandings and therapeutic considerations in 2020, Int. J. Mol. Sci. 21 (2020) 7794, https://doi.org/10.3390/ijms21207794.
[47] M.B. Schmidt, E.H. Chen, S.E. Lynch, A review of the effects of insulin-like growth factor and platelet derived growth factor on in vivo cartilage healing and repair, Osteoarthritis Cartilage 14 (2006) 403–412, https://doi.org/10.1016/j.joca.2005.10.011.
[48] D. Delgado, A. Garate, H. Vincent, A.M. Bilbao, R. Patel, N. Fiz, S. Sampson, M. Sánchez, Current concepts in intraosseous platelet-rich plasma injections for knee osteoarthritis, J Clin Orthop Trauma 10 (2019) 36–41, https://doi.org/10.1016/j.jcot.2018.09.017.
[49] S.S. Liu, L.L. Xu, L.K. Liu, S.J. Lu, B. Cai, Platelet-rich plasma therapy for temporomandibular joint osteoarthritis: a randomized controlled trial, J. Cranio-Maxillo-Fac. Surg. 51 (2023) 668–674, https://doi.org/10.1016/j.jcms.2023.09.014.
[50] T.L. Krammer, S. Zeibig, W.C. Schrottmaier, A. Pirabe, S. Goebel, A.B. Diendorfer, H.P. Holthoff, A. Assinger, M. Hackl, Comprehensive characterization of platelet-enriched microRNAs as biomarkers of platelet activation, Cells 11 (2022) 1254, https://doi.org/10.3390/cells11081254.
[51] C. Shifu, Z. Yanqing, C. Yaru, J. Gu, fastp: an ultra-fast all-in-one FASTQ preprocessor, Bioinformatics 34 (2018) i884, https://doi.org/10.1093/bioinformatics/bty560. –i890.
[52] D. Kim, B. Langmead, SL Salzberg Hisat, A fast spliced aligner with low memory requirements, Nat. Methods 12 (2015) 357–360.
[53] S. Anders, P.T. Pyl, W. Huber, HTSeq—a Python framework to work with high-throughput sequencing data, Bioinformatics 31 (2015) 166–169, https://doi.org/10.1093/bioinformatics/btu638.
[54] A. Roberts, C. Trapnell, J. Donaghey, J.L. Rinn, L. Pachter, Improving RNA-Seq expression estimates by correcting for fragment bias, Genome Biol. 12 (2011) R22, https://doi.org/10.1186/gb-2011-12-3-r22.
[55] M.I. Love, W. Huber, S. Anders, Moderated estimation of fold change and dispersion for RNA-seq data with DESeq2, Genome Biol. 15 (2014) 550, https://doi.org/10.1186/s13059-014-0550-8.